Control of Surface Plasmon Localization via Self-Assembly of Silver Nanoparticles along Silver Nanowires

ARTICLE *in* JOURNAL OF THE AMERICAN CHEMICAL SOCIETY · JANUARY 2009

Impact Factor: 12.11 · DOI: 10.1021/ja807218e · Source: PubMed

9 AUTHORS, INCLUDING:

Silvia P. Centeno
University of Malaga
22 PUBLICATIONS **350** CITATIONS
SEE PROFILE

Bert F Sels
University of Leuven
187 PUBLICATIONS **5,545** CITATIONS
SEE PROFILE

Hiroshi Uji-i
University of Leuven
104 PUBLICATIONS **2,855** CITATIONS
SEE PROFILE

J|A|C|S
COMMUNICATIONS

Published on Web 12/02/2008

Control of Surface Plasmon Localization via Self-Assembly of Silver Nanoparticles along Silver Nanowires

M. Linh Tran,[†] Silvia P. Centeno,[†] James A. Hutchison,[†] Hans Engelkamp,[†,||] Duoduo Liang,[‡] Gustaaf Van Tendeloo,[‡] Bert F. Sels,[†] Johan Hofkens,[†] and Hiroshi Uji-i*,[†]

Department of Chemistry and Center for Surface Chemistry and Catalysis, Katholieke Universiteit Leuven, Celestijnenlaan 200 F, B-3001 Leuven, Belgium, and EMAT (Electron Microscopy for Materials Science) Universiteit Antwerpen, Groenenborgerlaan 171, 2020 Antwerpen, Belgium

Received September 11, 2008; E-mail: Hiroshi.ujii@chem.kuleuven.be

Engineering of the optoelectronic properties of hybrid metal−metal nanostructures is of significant importance for the design of linear/nonlinear optical devices, bio/chemical sensors and substrates for surface-enhanced Raman scattering (SERS) or surface-enhanced fluorescence spectroscopy.[1]

Metal nanoparticles (NPs) exhibit strong optical responses due to the collective excitation of the electron gas in the conduction band of the metal, localized surface plasmon resonances (LSPRs).[2] The LSPR frequency depends strongly on the element, size, and shape of the NP.[2,3] In hybrid structures of NPs, coupling of LSPRs can create regions of concentrated fields, "hot-spots", in the gaps between particles, important for high-sensitivity surface enhanced spectroscopy and high-resolution microscopy. A fundamental challenge remains the facile construction of hybrid structures exhibiting spatially controlled LSPR hot-spots.[4] In random NP assemblies, the hot-spot position is difficult to control and more complicated lithographic techniques must be employed to get reproducible hot-spot distributions.

Here, we communicate the remarkable optical properties of a hybrid structure consisting of a silver nanowire (NW) densely decorated with silver nanoparticles (NPs). Under wide-field (WF) illumination, well-separated and fairly regular spots of localized emission/scattering are observed along the NW. The phenomenon is attributed to collective interactions of the LSPRs of the many NPs with propagating surface plasmons on the NW. The structure represents an unusual example of a random self-assembly process resulting in a hybrid displaying LSPR hot-spots at fairly regular intervals.

The silver nanowires (NWs) used here were obtained using the well-established polyol synthesis.[5] The ratio of $AgNO_3$ and PVP (poly(vinyl pyrrolidone)) was optimized so that the reaction suspension contained a large amount of silver nanocubes of ∼30 nm length and a small fraction of NWs with 2−30 μm length and 50−100 nm diameter. The reaction suspension was then used directly for all experiments without further treatment, such as centrifugation or filtering. Samples were prepared either by drop-casting or spin-coating the suspension onto a substrate (carbon grid or glass coverslip). Optical properties of the NWs were investigated using a WF luminescence microscope equipped with a high-sensitivity cooled CCD camera and using circularly polarized, continuous wave laser light of 488, 532, 633, or 660 nm. The WF images presented in Figures 1 and 2 were recorded using 532 nm excitation. Further details of the experimental methods are provided in Supporting Information (SI).

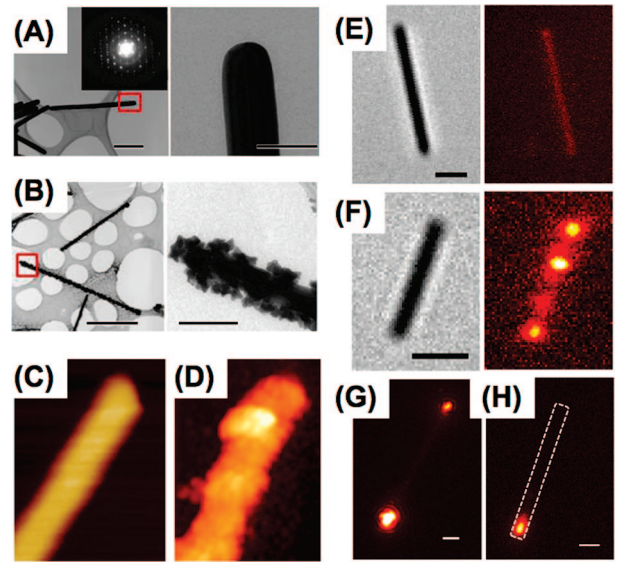

Figure 1. Typical TEM images of the spin-coated (A) and the drop-cast samples (B) on TEM carbon grids. The images on the right are zoomed areas indicated with squares in the images on the left. Scale bar is 500 and 100 nm for the left and right images, respectively. Inset in panel A is the electron diffraction image of the spin-coated NW. AFM images of samples prepared on clean coverslips are shown in panel C for a spin-coated NW (1.2×1.6 μm^2) and panel D for a drop-cast NW (1.0×1.3 μm^2). (E, F) Optical transmission (left) and wide-field luminescence (right) images for a spin-coated NW and a drop-cast NW, respectively. Scale bars are 1 μm. (G, H) The plasmon waveguide properties of a spin-coated and a drop-cast NW, respectively. The laser light was focused at the bottom end of the NWs. Scale bar is 1 μm.

Figures 1A and 1B show typical transmission electron microscopy (TEM) images of the spin-coated and drop-cast NWs, respectively, on carbon grids. While the spin-coated NWs have smooth surfaces, the surfaces of the NWs prepared by the drop-casting method are densely covered with objects of ca. tens of nanometers in dimension. The TEM experiments indicate that the observed heterostructures on the drop-cast NW surfaces are external to the NW structure and not intrinsic to the NW growth. Electron diffraction indicates the NW is a single crystal (inset Figure 1A and Figure S1, SI), while the small objects are poly crystalline and partially oxidized according to energy dispersive spectroscopy. Similar features are confirmed on NWs prepared on glass coverslips in the same manner, using atomic force microscopy (AFM) (Figure 1C,D).

The optical properties of NWs prepared by the spin-coating and drop-casting methods are also strikingly different. The spin-coated NWs show no particular features in the optical transmission image and almost no emission/scattering upon wide-field illumination

[†] Katholieke Universiteit Leuven.
[‡] Universiteit Antwerpen.
[||] Radboud University Nijmegen.

10.1021/ja807218e CCC: $40.75

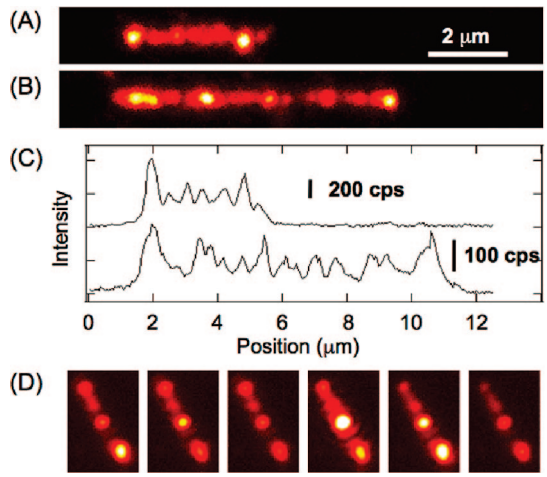

Figure 2. (A, B) WF images of two drop-cast NWs. (C) Line profiles along the NWs long axis in panels A and B. (D) A set of snapshots of the WF image of a drop-cast NW after (from left) 0, 1.5, 2.5, 6.5, 7.5, and 9.5 s.

(Figure 1E). When one end of the NW is excited with a diffraction limited laser focus, the NWs exhibit a plasmon waveguide effect due to coupling of light energy to the electron gas in the NW to form propagating surface plasmon polaritons (SPPs). In single crystalline NWs of these dimensions, SPPs can propagate over tens of micrometers and may be scattered as free photons at the opposite end of the NW, as observed in Figure 1G.[6]

For the NWs prepared by drop-casting, the dense assembly of NPs at the surface completely disturbs SPPs propagation along the NW (Figure 1H and Figure S2, SI). Under wide field illumination a remarkably different optical effect is observed. The drop-cast NWs show clear emission/scattering spots occurring along the long axis of the structure with reasonably regular spacing between spots (Figure 1F).

Figure 2 shows two more drop-cast NWs under WF illumination (A, B) with intensity profiles taken along the long axis (C). The average distances between spots are measured to be 544 ± 120 and 665 ± 215 nm for the NWs in Figure 2 panels A and B, respectively. While the average distance between spots varies from NW to NW, the position of the spots on a single NW are insensitive to excitation wavelength in the range 488−660 nm (Figure S5, SI). The total intensity of spots on a NW is wavelength dependent however, with highest intensity observed for 532 nm excitation and almost no emission observed with 660 nm excitation. Interestingly, the intensity of the emission/scattering spots fluctuates over time, as shown in the series of WF images in Figure 2D (see also intensity trajectories in Figure S3 and a movie in the SI). No clear correlation between the intensity fluctuations of different spots on a single NW can be established.

Spectrally resolving the emission spots shows that the dominant contribution is spectrally broad plasmon emission with initially a small contribution of SERS of PVP. The observation of localized emission/scattering suggests that the spots are indeed LSPR hot-spots in which high local fields occur. The images presented herein were recorded after the Raman signal was almost bleached (Figure S4, SI).

The influence of surface roughness/adsorbed NPs on plasmon propagation in thin metal films is well-known.[7] More recently the interconversion of free photons and propagating SPPs has been observed at points of NP adsorption on NWs with low NP coverage.[8] In the case of dense decoration of NPs here however, the number of emission spots is clearly much less than the number of adsorbed NPs. TEM images (Figure 1B) show that even NP clusters on the wire surface are separated by less than <100 nm, whereas the hot-spot spacing is usually >500 nm. These facts are suggestive of a collective interaction between the LSPRs of the many NPs and SPPs of the NW, resulting in the widely spaced hot-spots. At the same time, the fact that hot-spot spacing is not perfectly regular and is wavelength independent suggests that a resonance mode involving the whole structure is unlikely.

In summary, silver NWs densely decorated with silver NPs, self-assembled by a simple wet-chemical method, exhibit well-separated and fairly regular hot-spots of LSPRs. The detailed mechanism of the phenomenon and its dependence on metal composition and NP size/shape is under investigation.

Acknowledgment. Financial support of the "Fonds voor Wetenschappelijk Onderzoek FWO" (Grant G.0366.06), the KULeuven Research Fund (GOA 2006/2, Centers of Excellence CECAT and INPAC, CREA2007), and the Federal Science Policy of Belgium (IAP-VI/27) is gratefully acknowledged.

Supporting Information Available: Experimental procedures, emission spectra, intensity trajectories, additional WF images and a movie. This material is available free of charge via Internet at http://pubs.acs.org.

References

(1) (a) Barnes, W. L.; Dereux, A.; Ebbesen, T. W. *Nature* **2003**, *424*, 824–830. (b) Lippitz, M.; van Dijk, M. A.; Orrit, M. *Nano Lett.* **2005**, *5*, 799–802. (c) Anker, J. N.; Hall, W. P.; Lyandres, O.; Shah, N. C.; Zhao, J.; Van Duyne, R. P. *Nat. Mater.* **2008**, *7*, 442–453. (d) Habuchi, S.; Cotlet, M.; Gronheid, R.; Dirix, G.; Michiels, J.; Vanderleyden, J.; De Schryver, F. C.; Hofkens, J. *J. Am. Chem. Soc.* **2003**, *125*, 8446–8447. (e) Qian, X.-M.; Nie, S. M. *Chem. Soc. Rev.* **2008**, *37*, 912–920. (f) Kneipp, J.; Kneipp, H.; Kneipp, K. *Chem. Soc. Rev.* **2008**, *37*, 1052–1060.
(2) Kreibig, U.; Vollmer, M. *Optical Properties of Metal Clusters*; Springer: Berlin, 1994.
(3) (a) Okamoto, H.; Imura, K. *J. Mater. Chem.* **2006**, *16*, 3920–3928. (b) Félidj, N.; Grand, J.; Laurent, G.; Aubard, J.; Lévi, G.; Hohenau, A.; Galler, N; Aussenegg, F. R.; Krenn, J. R. *J. Chem. Phys.* **2008**, *128*, 094702.
(4) (a) Ueno, K.; Juodkazis, S.; Mizeikis, V.; Sasaki, K.; Misawa, H. *Adv. Mater.* **2008**, *20*, 26–30. (b) Laurent, G.; Félidj, N.; Grand, J.; Aubard, J.; Lévi, G.; Hohenau, A.; Krenn, J. R.; Aussenegg, F. R. *J. Microsc.* **2008**, *229*, 189–196.
(5) (a) Sun, Y. G.; Xia, Y. *Science* **2002**, *298*, 2176–2179. (b) Wiley, B.; Sun, Y. G.; Xia, Y. *Acc. Chem. Res.* **2007**, *40*, 1067–1076.
(6) (a) Dickson, R. M.; Lyon, L. A. *J. Phys. Chem. B* **2000**, *104*, 6095–6098. (b) Sanders, A. W.; Routenberg, D. A.; Wiley, B. J.; Xia, Y.; Dufresne, E. R.; Reed, M. A. *Nano Lett.* **2006**, *6*, 1822–1826.
(7) (a) Lyon, L. A.; Peña, D. J.; Natan, M. J. *J. Phys. Chem. B* **1999**, *103*, 5826–5831. (b) Raether, H. *Surf. Sci.* **1983**, *125*, 624–634.
(8) Knight, M. W.; Grady, N. K.; Bardhan, R.; Hao, F.; Nordlander, P.; Halas, N. J. *Nano Lett.* **2007**, *7*, 2346–2350.

JA807218E